THE JOURNAL OF BIOLOGICAL CHEMISTRY VOL. 291, NO. 22, pp. 11820–11828, May 27, 2016

The Stability and Expression Level of Bok Are Governed by Binding to Inositol 1,4,5-Trisphosphate Receptors*

Received for publication, December 17, 2015, and in revised form, April 5, 2016 Published, JBC Papers in Press, April 6, 2016, DOI 10.1074/jbc.M115.711242

Jacqualyn J. Schulman, Forrest A. Wright, Xiaobing Han, Eric J. Zluhan, Laura M. Szczesniak, and Richard J. H. Wojcikiewicz[1]

From the Department of Pharmacology, SUNY Upstate Medical University, Syracuse, New York 13210

Bok is a member of the Bcl-2 protein family that governs the intrinsic apoptosis pathway, although the role that Bok plays in this pathway is unclear. We have shown previously in cultured cell lines that Bok interacts strongly with inositol 1,4,5-trisphosphate receptors (IP_3Rs), suggesting that it may contribute to the structural integrity or stability of IP_3R tetramers. Here we report that Bok is similarly IP_3R-assocated in mouse tissues, that essentially all cellular Bok is IP_3R bound, that it is the helical nature of the Bok BH4 domain, rather than specific amino acids, that mediates binding to IP_3Rs, that Bok is dramatically stabilized by binding to IP_3Rs, that unbound Bok is ubiquitinated and degraded by the proteasome, and that binding to IP_3Rs limits the pro-apoptotic effect of overexpressed Bok. Agents that stimulate IP_3R activity, apoptosis, phosphorylation, and endoplasmic reticulum stress did not trigger the dissociation of mature Bok from IP_3Rs or Bok degradation, indicating that the role of proteasome-mediated Bok degradation is to destroy newly synthesized Bok that is not IP_3R associated. The existence of this unexpected proteolytic mechanism that is geared toward restricting Bok to that which is bound to IP_3Rs, implies that unbound Bok is deleterious to cell viability and helps explain the current uncertainty regarding the cellular role of Bok.

Bok is a member of the Bcl-2 protein family that controls the intrinsic apoptosis pathway (1–3). Bok contains four Bcl-2 homology domains (BH1–4)[2] and shares greatest sequence homology with the pro-apoptotic proteins Bak and Bax (1–4). However, unlike Bak and Bax, which have clearly defined roles in mediating mitochondrial outer membrane permeabilization (5, 6), the cellular role of Bok is unclear. Key observations that pertain to our current understanding of the function of Bok are (i) that the atypical C-terminal transmembrane (TM) domain of Bok localizes it to membranes of the endoplasmic reticulum (ER) and Golgi (7), (ii) that Bok over-expression leads to apoptosis (7–10) if Bak or Bax are present (7), indicating that Bok lies upstream of Bak and Bax, (iii) that $Bok^{-/-}$ mice are phenotypically normal (4, 11, 12), while $Bax^{-/-}Bak^{-/-}$ mice exhibit multiple severe defects (1), indicating that Bok cannot substitute for Bak and Bax, and (iv) that ER stress-induced apoptosis (13) can be suppressed in $Bok^{-/-}$ mouse cells *in vitro* and *in vivo* (12), although this result has not been seen by all groups (7). Overall, these data suggest that Bok plays a very different role from Bax and Bak, and that it may participate in the pathway between ER stress and apoptosis.

Another intriguing facet of Bok cell biology is that it binds very strongly to inositol 1,4,5-trisphosphate (IP_3) receptors (IP_3Rs) (14), proteins that form tetrameric, IP_3-, and Ca^{2+}-gated Ca^{2+} channels in ER membranes and play a key role in vertebrate cell signaling (15, 16). Of the three mammalian IP_3R types, Bok binding is strongest to IP_3R1 and IP_3R2 (14) and the binding site for Bok can be localized to a regulatory hotspot within the IP_3R ARM3 domain, part of the region that links the N-terminal IP_3-binding domain to the C-terminal channel domain (14, 16). Bok binds via its BH4 domain, since deletion of that domain abolishes binding to IP_3R1 (14). Interestingly, Bcl-2 also binds to IP_3R1 via its BH4 domain, albeit much less strongly than Bok and to a different IP_3R region (17–19). Nevertheless, Bcl-2 binding modulates IP_3R-mediated Ca^{2+} mobilization (17–19) and a peptide derived from the binding site in IP_3R1 reverses the suppressive effect of Bcl-2 on Ca^{2+} signaling and apoptosis (17, 20). In contrast, Bok binding does not appear to dramatically alter the Ca^{2+}-mobilizing function of IP_3Rs, but does protect IP_3Rs against proteolysis within the ARM3 domain *in vitro* and *in vivo*, apparently by steric hindrance of protease access (14).

Here we report that Bok stability is highly dependent upon binding to IP_3Rs and that "free" (non-IP_3R bound) Bok is ubiquitinated and is degraded by the proteasome. This novel mechanism restricts cellular Bok to that which is bound to IP_3Rs, implies that unbound Bok is deleterious to cell viability, and helps explain the current lack of clarity regarding the cellular role of Bok.

Experimental Procedures

Materials—αT3 cells and HEK 293T cells were cultured as described (14). Antibodies raised in rabbits were: anti-IP_3R1 (21), anti-erlin2 (22), anti-IP_3R1–3 (23), anti-HA epitope (24), anti-Mcl-1 D35A5, anti-Bcl-xL 54H6, anti-Bcl-2 50E3, anti-caspase-3 9662, and anti-poly (ADP-ribose) polymerase (PARP) 9542 (Cell Signaling Technology), anti-Bak 06–536 (Millipore), anti-Bax N-20 (Santa Cruz Biotechnology Inc.), and anti-Bok,

* This work was supported by National Institutes of Health Grant DK049194 and the Carol M. Baldwin Breast Cancer Research Fund. The authors declare that they have no conflicts of interest with the contents of this article. The content is solely the responsibility of the authors-and does not necessarily represent the official views of the National Institutes of Health.

[1] To whom correspondence should be addressed: Dept. of Pharmacology, SUNY Upstate Medical University, 750 E. Adams St., Syracuse, NY 13210. Tel.: 315-464-7956; Fax: 315-464-8014; E-mail: wojcikir@upstate.edu.

[2] The abbreviations used are: BH, Bcl-2 homology; IP_3, inositol 1,4,5-trisphosphate; IP_3R, inositol 1,4,5-trisphosphate receptor; ER, endoplasmic reticulum; PARP, poly (ADP-ribose) polymerase; UPP, ubiquitin-proteasome pathway; TM, transmembrane; CHX, cycloheximide; GnRH, gonadotropin-releasing hormone; IP, immunoprecipitation; PEI, polyethylenimine; MD, molecular dynamics.

raised against amino acids 19–32 of mouse Bok (4, 7). Mouse monoclonal antibodies were: anti-ubiquitin clone FK2 (BioMol International), anti-HA epitope clone HA11 (Covance), anti-FLAG epitope clone M2 (Sigma), and anti-p97 (Research Diagnostics Inc.). Horseradish peroxidase-conjugated secondary antibodies, gonadotropin-releasing hormone (GnRH), *N*-ethylmaleimide, protease inhibitors, Triton X-100, CHAPS, cycloheximide (CHX), thapsigargin, and forskolin were purchased from Sigma. DTT, Precision Plus^{TM} Protein Standards, and SDS-PAGE reagents were from Bio-Rad. Protein A-Sepharose CL-4B was from GE Healthcare. MG132 was from Biomol. Staurosporine was from Enzo Life Sciences. Linear, MW~25,000 polyethylenimine (PEI) was from Polysciences Inc.

Cell Lysis, Immunoprecipitation (IP), and SDS-PAGE—To prepare lysates, cells or brain tissues were harvested with ice-cold lysis buffer containing either 1% CHAPS or 1% Triton X-100 (14). CHAPS was used for all experiments involving IP, except when exogenous Bok ubiquitination was assessed, when cells were harvested with DTT-free Triton X-100 lysis buffer supplemented with 5 mM *N*-ethylmaleimide, followed by addition of 5 mM DTT 30 min later (25). Lysates were incubated on ice for 30 min and clarified by centrifugation at 16,000 × *g* for 10 min at 4 °C. For IP, clarified lysates were incubated with antisera and Protein A-Sepharose CL-4B for ~16 h at 4 °C, and IPs were washed thoroughly with lysis buffer, were resuspended in gel-loading buffer, were incubated at 37 °C for 30 min or 100 °C for 3 min, were subjected to SDS-PAGE, and proteins were transferred to nitrocellulose for probing as described (14).

Analysis of Exogenous Bok in HEK and HeLa Cells—Vectors encoding mouse Bok tagged at the N terminus with a triple FLAG epitope (3F-Bok) and mouse IP_3R1 tagged at the C terminus with an HA epitope have been described (14). Additional constructs were created encoding 3F-Bok-HA (3F-Bok with an HA epitope, GYPYDVPDYAG, added to the C terminus), 3F-Bak (14), and untagged mouse Bok inserted between the KpnI/BglII sites of pCAG (26). HEK 293T cells seeded at 4.5 × 10^5/9.6 cm^2 well, were transfected ~24 h later with 0.125–2.125 μg cDNAs and 6 μl of 1 mg/ml PEI (pre-mixed in 50 μl of serum-free culture medium), and ~24 h later were harvested with ~ 0.4 ml/well lysis buffer. HeLa cells were seeded at 7 × 10^5/9.6 cm^2 well, were transfected ~24 h later with 0.5 μg of cDNAs and 3.5 μl of Lipofectamine (Invitrogen), and ~24 h later were harvested with ~ 0.2 ml/well lysis buffer.

Generation and Analysis of IP_3R1 Knock-out (KO) Lines—The CRISPR/hCas9 system (27) was used to target exons within the mouse IP_3R1 gene and create αT3IP_3R1KO cell lines as described (25). Oligonucleotides targeting exons 5 or 13 (GGTGCGGAGTATCGATTCAT and GCACCTCCACGCAGAGTCGT, respectively) were introduced into αT3 cells and clones were screened by immunoblotting with anti-IP_3R1 (25). Of the cell lines screened, ~25% lacked IP_3R1, and 2 lines for each targeted exon were characterized further with essentially identical results. Cells (10^6/9.6 cm^2 well) were transiently transfected with IP_3R1HA constructs (0.25–1.2 μg of cDNAs and 6 μl of 1 mg/ml PEI) and were harvested 48 h later.

Measurement of mRNA Levels—RNA was extracted using the RNeasy Mini Kit (Qiagen) and was reverse transcribed into cDNA using the Reverse Transcription System (Promega). qRT-PCR was performed using the forward primer GATGGACGGATGTCCTCAAG and the reverse primer TCTCTGGCAACAACAGGAAG, a Taq master mix developed in-house containing SYTO-82 (Molecular Probes), 3 mM $MgCl_2$ and TaqDNA Polymerase (Thermo Fisher), a Stratagene MX3000P real time qPCR thermal cycler, and the following PCR cycling parameters: 10 min at 95 °C, followed by 40 cycles of 95 °C for 30 s, 55 °C for 30 s, and 72 °C for 30 s. Results were analyzed by normalizing to the housekeeping genes ribosomal protein S18, peptidylprolyl isomerase A, and hypoxanthine phosphoribosyltransferase 1, using the $2^{-\Delta\Delta CT}$ method (28).

Homology Modeling and Molecular Dynamics (MD) Simulations—The human Bok protein sequence (NCBI accession number NP_115904.1) was modeled using human Bax (PDB entry 1F16) and human Bak (PDB entry 2YV6) as templates and the Modeler v9.12 program (29) with the very slow refinement setting for MD optimization. The N-terminal 21 residues and C-terminal 10 residues of Bok were intentionally not modeled, as the N-terminal is disordered or absent in the Bax and Bak structures and the C terminus does not align with Bax and Bak. The best of 50 models identified by the GA341 and DOPE score functions was then further refined using the loop-refine script to create a set of 20 models with modified loop conformations. The model with the lowest MOLPDF score was then selected as the final Bok model.

To assess the structural effects of mutating Leu^{34} to Gly, RosettaBackrub (30) was first used to create a model of Bok^{L34G}, which revealed little effect on the overall structure of the residue 24–42 α-helical region, but significant shifts in the position of some amino acid side chains. MD simulations of this region of Bok^{WT} and Bok^{L34G} were then performed using the Gromacs 4.5.5 package (31) and Amber99SB force field (32). Each peptide was solvated in an octahedral box filled with TIP3P water and the net charges were neutralized with 0.15 M NaCl. The PME method was used to treat long-range electrostatic interactions, a cutoff of 10Å was used for the Coulomb energy and Van Der Waals interactions, the system was energy minimized until reaching 1000 kJ/mol/nm, and then equilibrated for 100 ps using the v-rescale method at 300 K, followed by pressure equilibration for 100 ps using the Parrinello-Rahman method at 300 K, and the LINCS algorithm was applied to constrain all bond lengths. In the final 10-ns MD simulation, the time step was 2 fs, and structures were saved every 2 ps.

Data Analysis—All experiments were repeated at least once (n = the number of independent experiments) and representative images of gels and traces are shown. Quantitated data are graphed as mean ± S.E. when $n \geq 3$ or mean ± range when $n = 2$.

Results

Bok-IP_3R1 Binding in Vivo and the Origin of Bok Variants—We have shown previously, via IP, that Bok binds tightly to IP_3Rs in various cultured cell lines (14). Examination of mouse brain shows that such binding also occurs *in vivo* (Fig. 1), since IP of IP_3R1 from brain cerebral cortex and hippocampus lysates specifically isolates Bok (*lanes 2* and *3*). Further, anti-IP_3R1 depleted the vast majority of both IP_3R1 and Bok from the

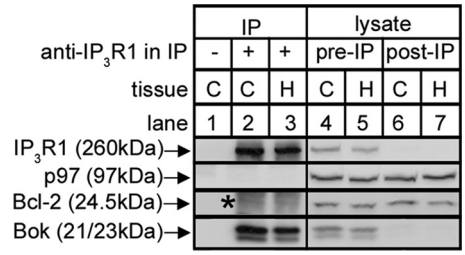

FIGURE 1. **Co-IP of Bok with IP_3R1 in mouse brain tissues.** Mouse brain cerebral cortex (*C*) and hippocampus (*H*) lysates were incubated without or with anti-IP_3R1, and IPs (*lanes 1–3*) and lysates (either pre- or post-IP; *lanes 4–7*) were subjected to SDS-PAGE and probed for the proteins indicated. p97 and Bcl-2 served as negative controls that did not co-IP and show that Bok co-IP is specific. Co-migrating IgG light chain seen in the Bcl-2 probe is indicated by the *asterisk*.

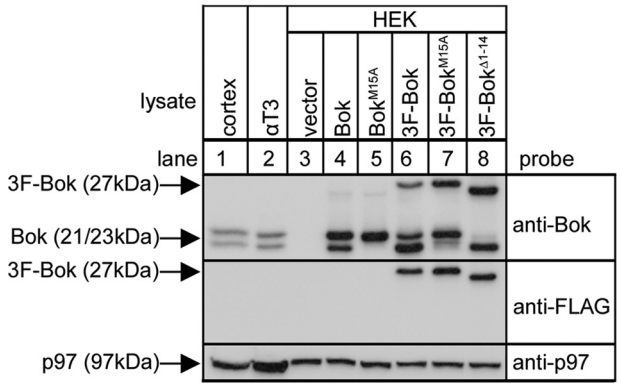

FIGURE 2. **Analysis of the origin of Bok variants.** Lysates from mouse brain cerebral cortex and αT3 cells (*lanes 1* and *2*) and HEK cells transfected to express the constructs indicated (*lanes 3–8*) were subjected to SDS-PAGE and probed with anti-Bok, anti-FLAG and anti-p97 as a loading control.

lysates (compare *lanes 4* and *5* with *6* and *7*), indicating that essentially all Bok is IP_3R1-associated.

It is noteworthy that in mouse tissues and cell lines (Figs. 1 and 2, *lanes 1–2*) (14), anti-Bok, which is raised against amino acids 19–32 of mouse Bok (Fig. 3*A*), recognizes two species (at 21 and 23 kDa). Bands at 21 and 23 kDa were also seen after expression of exogenous Bok from mouse Bok cDNA in HEK cells (Fig. 2, *lane 4*). The existence of 21- and 23-kDa bands appears to be due to alternative translation initiation (33, 34), since mutation of the second AUG codon in the Bok coding region (that encodes Met^{15}) blocks formation of the 21-kDa band (*lane 5*). Interestingly, the 3F-Bok construct (Fig. 3*A*) used previously to map the Bok-IP_3R interaction (14) generated anti-Bok-immunoreactive bands at 27, 23, and 21 kDa (*lane 6*), with the anti-FLAG immunoreactive band at 27 kDa corresponding to full-length 3F-Bok, and the bands at 23 and 21 kDa corresponding to untagged Bok starting at Met^1 or Met^{15}. Again, evidence for alternative translation initiation comes from the observation that 3F-Bok^{M15A} does not generate the 21kDa band (lane 7) and that 3F-$Bok^{\Delta 1-14}$ (Fig. 3*A*) does not generate the 23kDa band. Thus, Bok mRNA appears to be translated using either Met^1 or Met^{15} as the initiation codon, perhaps because of "leaky scanning" (33, 34) during the initiation of translation.

Resolution of the Determinants of Bok Binding—To resolve the determinants of Bok binding to IP_3R1 we made a series of truncations and point mutations in the vicinity of the BH4 domain (Fig. 3*A*), analyzed the ability of these constructs to interact with IP_3R1HA (Fig. 3*D*), and generated molecular models to gain insight into the effects of these modifications on the structure of Bok (Fig. 3, *B* and *C*). The Bok model (Fig. 3*B*), which is based on Bax and Bak, indicates that the BH4 domain (bright pink) is located within the first α-helical region of Bok (residues 24–42), which lies in an accessible cleft. Sequential truncations within this α-helical region (Fig. 3, *A* and *C*) confirmed the role for the BH4 domain in mediating binding, since 3F-$Bok^{\Delta 1-27}$ and 3F-$Bok^{\Delta 1-32}$ bound well to IP_3R1HA, but 3F-$Bok^{\Delta 1-39}$ did not (Fig. 3*D*, *lanes 2–5*). Surprisingly, it does not appear that it is specific residues in the BH4 domain that mediate binding, but rather the overall structure of the domain, as 3F-Bok^{A34-36} and 3F-Bok^{A37-38} bind well, but 3F-Bok^{A34-38} does not (Fig. 3*D*, *lanes 6–8*). To confirm this idea, we mutated Leu^{34} to Gly, since adjacent Gly residues destabilize α-helices (35) and a previous study has shown that a di-Gly mutation in the BH4 domain of Bcl-2 blocks binding to IP_3Rs (36). This mutation distorts the BH4 domain of Bok, as indicated by MD simulation (Fig. 3*C*), and indeed, the 3F-Bok^{L34G} mutant does not bind to IP_3R1HA (Fig. 3*D*, *lane 9*).

Exogenous Bok Expression Is Dependent upon Binding to IP_3R1—We noted in certain experiments using the co-transfection approach shown in Fig. 3*D*, that binding-deficient Bok mutants did not express as well as constructs that bound strongly to IP_3R1HA. To examine this more carefully we monitored the effect of IP_3R1HA on 3F-Bok expressed from a range of cDNA amounts (Fig. 4*A*). This revealed that IP_3R1HA dramatically enhanced 3F-Bok expression, particularly when the lowest amounts of 3F-Bok cDNA were used (*lanes 1–6*). This was truly because of binding to IP_3R1HA, because $IP_3R1HA^{\Delta 1-1903}$, which does not bind Bok (14), did not affect 3F-Bok expression, while $IP_3R1HA^{\Delta 1-1884}$, which does bind to Bok (14), enhanced 3F-Bok expression (Fig. 4*A*, *lanes 7–12*). The effect of binding to IP_3R1 on Bok expression was confirmed by the fact that the expression level of binding-deficient mutants (3F-Bok^{L34G} and 3F-Bok^{A34-38}) was essentially unaffected by co-expression of IP_3R1HA (Fig. 4*B*, *lanes 4* and *8*), while 3F-Bok^{WT} and 3F-Bok^{A34-36} expression was greatly enhanced (*lanes 2* and *6*).

CHX-chase experiments showed that 3F-Bok was turned over more rapidly in the absence of IP_3R1HA than in the presence of IP_3R1HA (Fig. 4*C*), indicating that Bok is unstable in the absence of IP_3R1, which in turn accounts for the low expression level. To probe the apparent degradation mechanism, cells were incubated with MG132, an inhibitor of the proteasome (Fig. 4*D*). This markedly increased 3F-Bok levels in the absence of IP_3R1HA (*lanes 3–6*), but had no effect on 3F-Bok levels when IP_3R1HA was present (*lanes 1* and *2*), indicating that "free" 3F-Bok is degraded by the proteasome. Conversely, the levels of 3F-Bak were unaffected by MG132 (*lanes 7* and *8*), showing that the increase seen for 3F-Bok is protein specific and not due to a generic effect on expression from the plasmid. Finally, the relatively rapid decline in 3F-Bok levels in the presence of CHX was partially blocked by MG132 (*lanes 9–13*), again implicating the proteasome in the turnover of free 3F-Bok.

To establish whether Bok is ubiquitinated, 3F-Bok-HA was immunoprecipitated from control and MG132-treated HEK

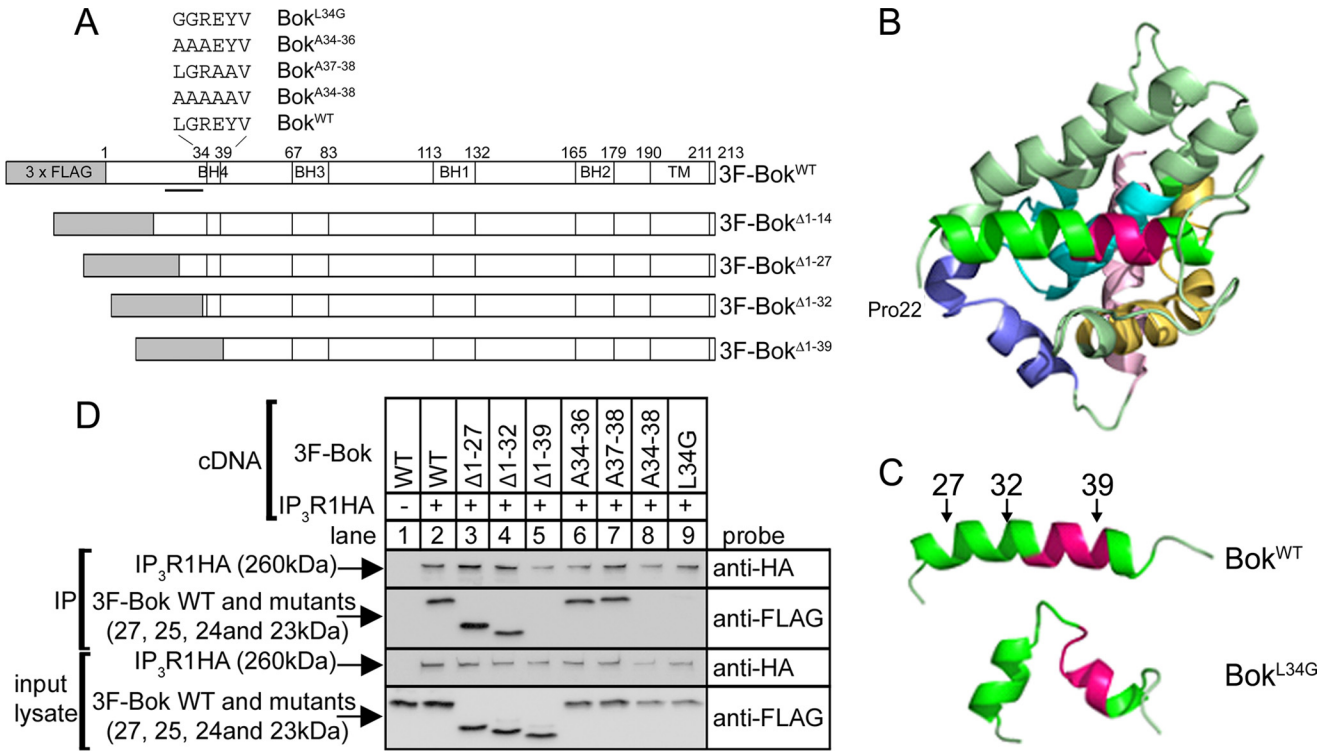

FIGURE 3. **Analysis of the determinants of Bok binding and molecular modeling.** *A*, 3F-Bok constructs used to define the region that binds to IP$_3$Rs. Shown are the N-terminal triple FLAG tag (*gray box*), the position of the BH1–4 domains (1–3, 14), the TM region, and the sequence of the mouse Bok BH4 domain (LGREYV), together with the mutants used to resolve the binding site. The anti-Bok epitope, residues 19–32 (4, 7), is indicated by the *black bar*. *B*, Bok homology model, based on Bax and Bak, showing the α-helical region (*bright green*, residues 24–42) that contains the BH4 domain (*bright pink*), and also the locations of the BH3 (*yellow*), BH1 (cyan), BH2 (*blue*) and TM (*light pink*) domains. The model starts at Pro^{22} and ends at Lys^{202} of Bok. *C*, models of the residue 24–45 region of Bok^{WT} and Bok^{L34G} after MD simulation for 10 ns. The positions of the BH4 domain (*bright pink*) and truncation points used in deletion mutants (*arrows*) are indicated. *D*, HEK 293T cells were transfected with cDNAs encoding 3F-Bok constructs and IP$_3$R1HA, were harvested 24 h later, lysates were incubated without or with rabbit anti-HA, and IPs and input lysates were subjected to SDS-PAGE and probed for IP$_3$R1HA and the 3F-Bok constructs.

cells and probed for ubiquitin. This revealed the presence of high molecular mass ubiquitinated species after MG132 treatment (Fig. 5, *lane 3*), that was not seen in control samples (*lanes 1* and *5*). Thus, ubiquitination of exogenous Bok appears to mediate its degradation.

Endogenous Bok Levels Are Dramatically Reduced by IP$_3$R1 Deletion—To determine whether endogenous Bok levels are also IP$_3$R-dependent, we examined αT3 cells, the cell type in which we originally discovered that endogenous Bok and IP$_3$R1 interact strongly (14), and in which IP$_3$R1 constitutes ~99% of total IP$_3$R content (22). Remarkably, CRISPR/Cas9-mediated deletion of IP$_3$R1 caused a dramatic decline in Bok levels (Fig. 6*A*), to ~2% of that seen in control cells (Fig. 6*B*), since the Bok immunoreactivity seen with 30 μg of IP$_3$R1KO cell lysate (*lane 1*) was equivalent to that seen with 0.5–1 μg of control cell lysate (*lanes 2* and *3*). The decline in Bok expression was totally specific, as the levels of other pertinent proteins were unaffected (Fig. 6*A*), and was not due to loss of Bok mRNA, the levels of which were not substantially different in control αT3 and αT3IP$_3$R1KO cells (Fig. 6*C*). Further, reintroduction of IP$_3$R1HA and IP$_3$R1HA$^{Δ1-1884}$, which bind Bok (14), into αT3IP$_3$R1KO cells caused a partial recovery of Bok expression, not seen with the binding-deficient construct IP$_3$R1HA$^{Δ1-1903}$ (Fig. 6*D*); it is likely that the recovery is only partial because of the relatively low transfection efficiency seen in αT3 cells (24, 25). This confirms that the Bok gene and mRNA are normal in αT3IP$_3$R1KO cells and indicates that Bok is degraded in the absence of IP$_3$R1. The degradation mechanism seems identical to that seen for exogenous 3F-Bok, since in αT3IP$_3$R1KO cells, endogenous Bok levels were enhanced by MG132 (Fig. 6*E*, *lanes 1–4*) and CHX-chase showed that endogenous Bok is rapidly degraded (*lanes 5–7*) in a MG132-sensitive manner (*lanes 8* and *9*); none of these changes were seen in control αT3 cells (Fig. 6*E*, *lanes 10–18*). It is perhaps surprising that treatment with MG132 only doubled the level of Bok in αT3IP$_3$R1KO cells (Fig. 6*E*, *lanes 1–4*) and that Bok levels did not approach the amount seen in control αT3 cells. This may be because MG132, in addition to inhibiting the proteasome, also causes ER stress and inhibits protein synthesis (12, 13). So, even though Bok degradation by the proteasome is blocked by MG132, so is the synthesis of new Bok, and only a modest increase in Bok levels are seen.

Binding to IP$_3$Rs Limits the Pro-apoptotic Effect of Overexpressed Bok—Since previous studies have shown that Bok overexpression triggers apoptosis (7–10), we examined whether binding to IP$_3$Rs is important for this effect by comparing the pro-apoptotic effects of overexpressed Bok^{WT} and Bok^{L34G} (which does not bind to IP$_3$Rs). Interestingly, we found that both Bok^{WT} and Bok^{L34G} trigger apoptosis, as indicated by enhanced caspase-3 and PARP cleavage, and remarkably, that Bok^{L34G} is more effective (Fig. 7, *lanes 2* and *3*). Under these conditions, some Bok^{WT} co-immunoprecipitates with endoge-

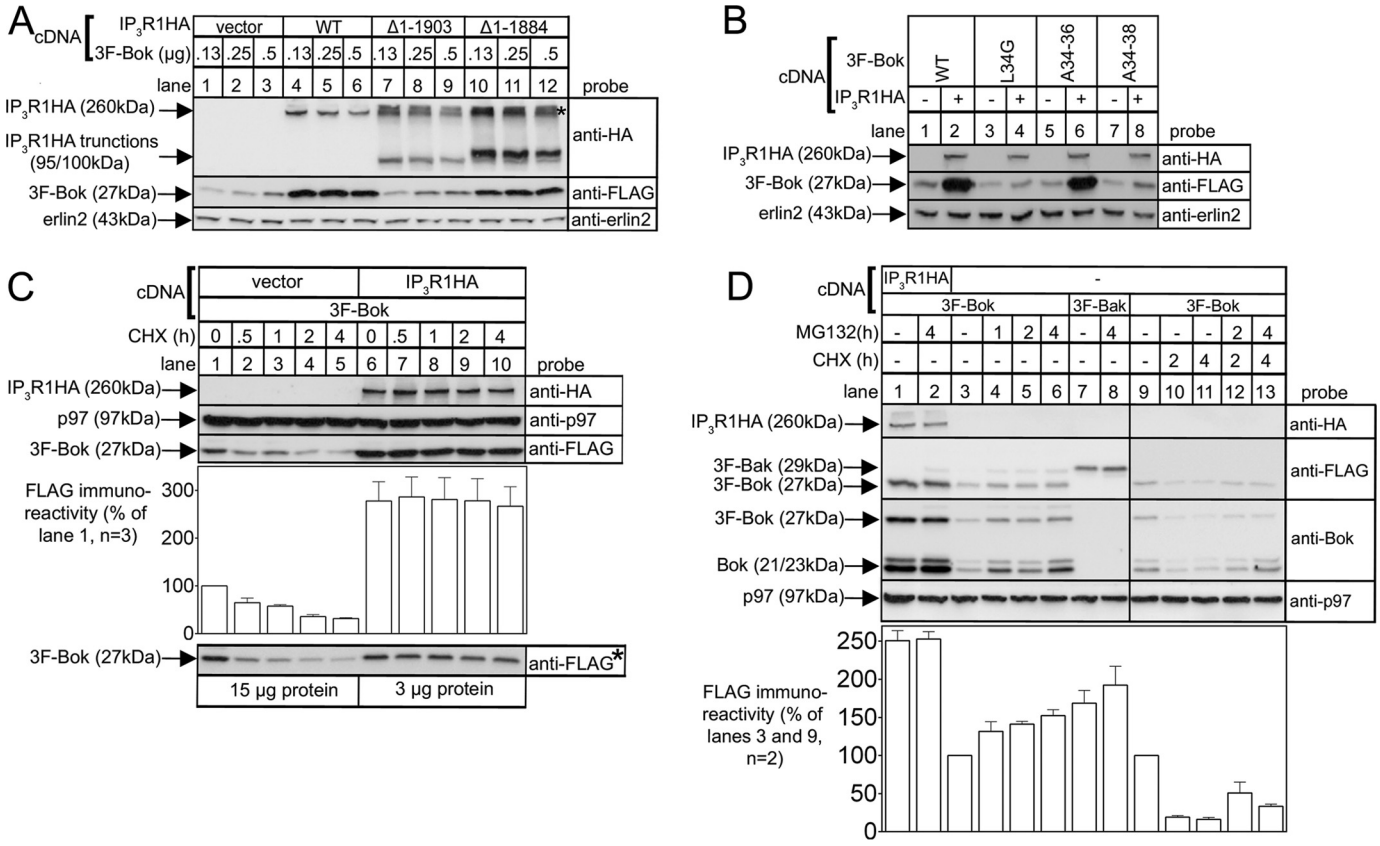

FIGURE 4. **Exogenous Bok expression is enhanced by IP$_3$R1 and is degraded by the ubiquitin-proteasome pathway when not bound to IP$_3$R1.** HEK cells were transfected to express various 3F-Bok and/or IP$_3$R1HA constructs, were incubated without or with 20 μg/ml CHX or 10 μM MG132 for the times indicated, were lysed, and were subjected to SDS-PAGE and probed as indicated. Erlin2 and p97 served as loading controls. The *histograms* show combined quantitated anti-FLAG immunoreactivity from multiple independent experiments. The *asterisk* in *panel A* marks the position in *lanes 7–12* of high molecular mass (ubiquitinated) species derived from the truncated IP$_3$R1HA constructs. The *asterisked image* in *panel C* was obtained by loading 15 μg and 3 μg of protein from vector- and IP$_3$R1HA-transfected cells, respectively, to demonstrate that the signal from IP$_3$R1HA-transfected cells is not saturated.

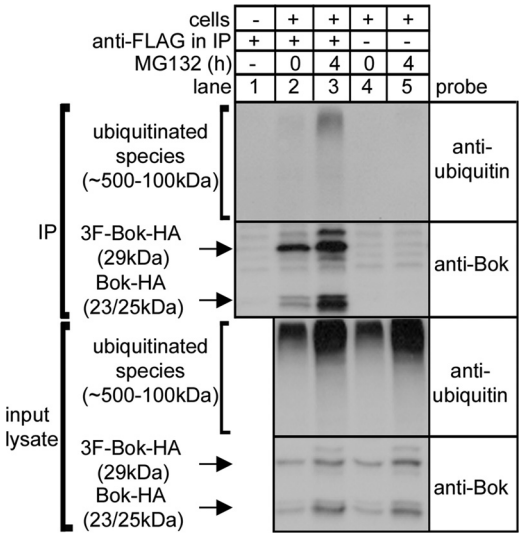

FIGURE 5. **Bok ubiquitination.** HEK cells transfected to express 3F-Bok-HA were incubated without or with 10 μM MG132, were lysed, were incubated without or with anti-FLAG, and IPs and input lysates were subjected to SDS-PAGE and probed as indicated.

nous IP$_3$Rs, while Bok^{L34G} remains completely free (*lower panels*; *lanes 2* and *3*). This indicates that it is not necessary for exogenous Bok constructs to bind IP$_3$Rs to be pro-apoptotic and, in fact, that the binding of Bok to IP$_3$Rs limits apoptosis, apparently by limiting the amount of free Bok. Thus, free Bok, rather than IP$_3$R-bound Bok, seems to be the trigger for apoptosis.

Stimuli Do Not Cause Release of Bok from IP$_3$R1—Various agents were added to αT3 cells to determine whether Bok release from IP$_3$R1 can be triggered, since that might cause Bok degradation and a decrease in cellular Bok levels. However, Fig. 8 (*lanes 5–13*) shows that neither the amount of Bok that co-IPs with IP$_3$R1, nor cellular Bok levels, were substantially altered by staurosporine, a kinase inhibitor that triggers apoptosis and causes caspase-3-mediated IP$_3$R1 cleavage (14–16), by forskolin, which triggers cAMP-dependent protein kinase-mediated phosphorylation of IP$_3$R1 (15) and Bok (37), or by thapsigargin, which inhibits ER Ca^{2+}-ATPase, depletes Ca^{2+} stores and leads to ER stress (12, 13). A slight but consistent decrease in Bok levels and co-IP was seen in response to GnRH (*lanes 1–4*), which triggers a robust increase in IP$_3$ levels, IP$_3$R1 activation, and proteasome-mediated IP$_3$R1 degradation (14, 24, 25). However, that decrease is most likely because Bok bound to IP$_3$R1 is degraded in unison with IP$_3$R1 (14), rather than because it is released from IP$_3$R1.

Discussion

Our data indicate that the stability and thus the expression level of Bok is highly dependent upon binding to IP$_3$Rs. This

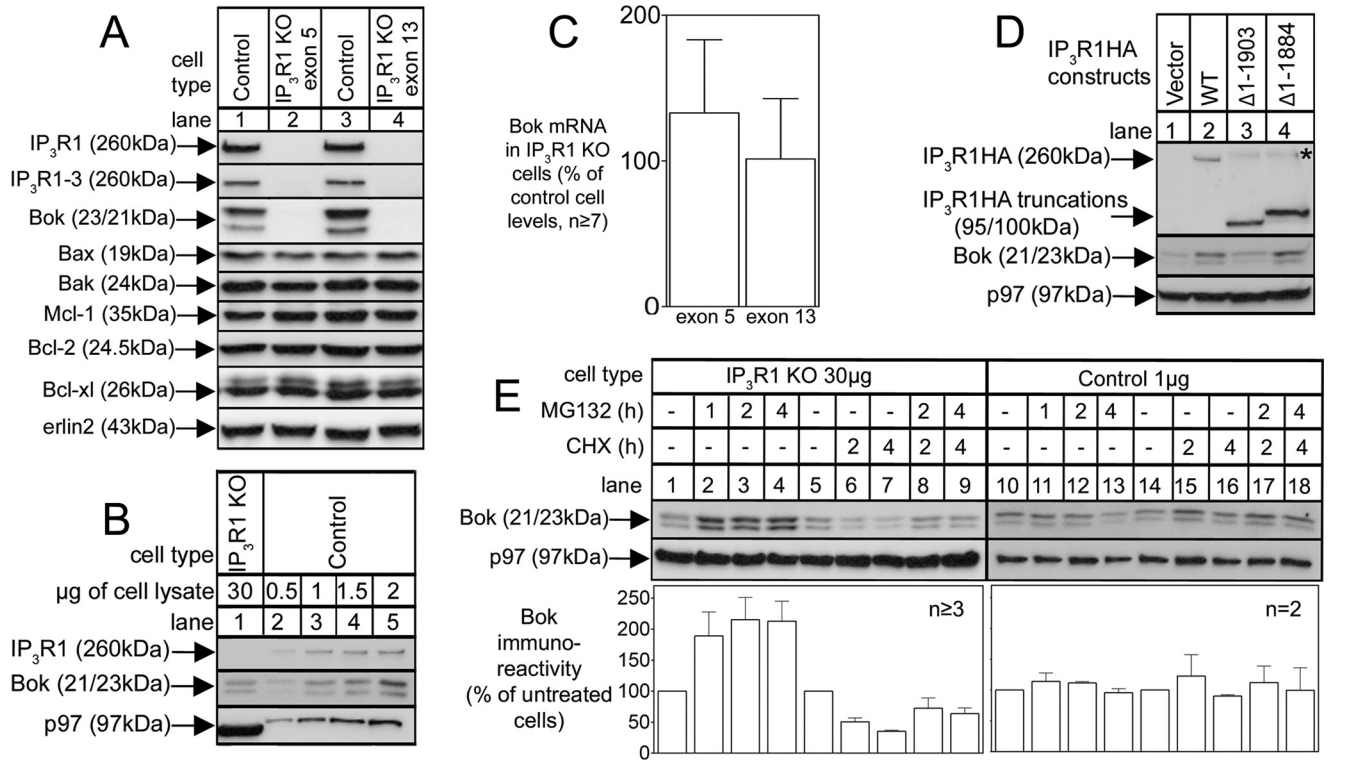

FIGURE 6. **Endogenous Bok is stabilized by IP$_3$R1.** *A*, levels of IP$_3$R1 and Bok and other pertinent proteins in lysates from αT3 control and IP$_3$R1KO cells obtained by targeting exon 5 (*lane 2*) and exon 13 (*lane 4*). *B*, comparison of Bok immunoreactivity in αT3 control and IP$_3$R1KO cells obtained by loading different amounts of cell lysate. *C*, Bok mRNA levels (normalized to peptidylprolyl isomerase A) in exon 5 and exon 13 targeted αT3IP$_3$R1KO cells, relative to the amount present in αT3 control cells. *D*, αT3 IP$_3$R1KO cells were transfected with cDNAs encoding the IP$_3$R1HA constructs indicated and cell lysates were probed for Bok. The *asterisk* marks the same species described in Fig. 4. *E*, αT3 control and IP$_3$R1KO cells were treated as indicated with 10 μM MG132 and 20 μg/ml CHX, and 1 μg and 30 μg, respectively, of cell lysates were probed for Bok. The histogram shows combined quantitated Bok immunoreactivity normalized to levels in untreated cells from multiple independent experiments. An exon 5-targeted clone was used for the experiments shown in *panels B*, *D*, and *E*, and erlin2, and p97 served as loading controls.

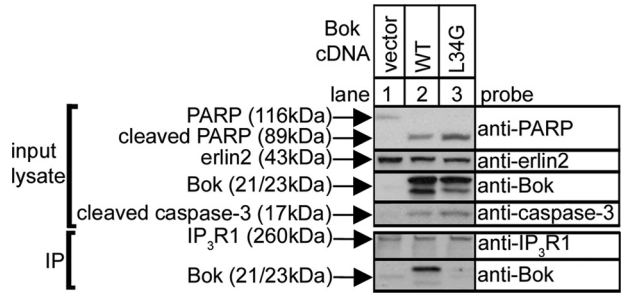

FIGURE 7. **Enhanced pro-apoptotic effects of Bok^{L34G}.** HeLa cells were transfected with pCAG-based vectors encoding Bok^{WT} and Bok^{L34G}, were harvested 24 h later, lysates were incubated with anti-IP$_3$R1, and input lysates and IPs were subjected to SDS-PAGE and probed for the proteins indicated.

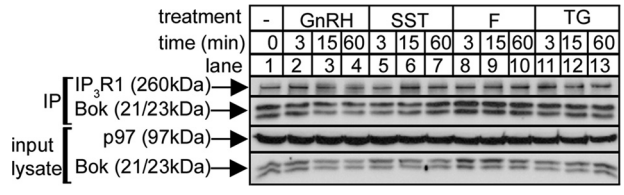

FIGURE 8. **Lack of effect of cell stimulation on the Bok-IP$_3$R1 interaction.** αT3 cells were incubated as indicated with 1 μM GnRH, 1 μM staurosporine (*SST*), 10 μM forskolin (*F*), and 1 μM thapsigargin (*TG*), and cell lysates and anti-IP$_3$R1 IPs were subjected to SDS-PAGE and probed in immunoblots for the proteins indicated.

was demonstrated by focusing on the interaction of both exogenous and endogenous Bok with IP$_3$R1, the most widely expressed and best understood IP$_3$R type (15, 16). When IP$_3$R1 is absent and, thus, the predominant binding site for Bok is also absent, "free" Bok appears to be degraded by the ubiquitin-proteasome pathway (UPP) (38).

The extent to which Bok levels are dependent upon IP$_3$R1 is quite remarkable, with the steady-state level of Bok in αT3IP$_3$R1KO cells being ~2% of that seen in control αT3 cells. Using pharmacological agents and GnRH, we were unable to trigger dissociation of the Bok-IP$_3$R1 complex and reduce endogenous Bok levels, suggesting that the extreme sensitivity of free Bok to the UPP is not a mechanism to control the levels of mature Bok that was once IP$_3$R-associated. Rather, it likely represents a cellular mechanism to disallow newly synthesized Bok from existing in a free form. It is important to note that Bok, like several other Bcl-2 protein family members, has a TM domain at the very C terminus (1–3, 7) and is thus a "tail anchored protein" (39–42). It is currently unclear how newly synthesized TA proteins are inserted into membranes, but for at least some it appears that the BAG6/Ubl4A/TRC35 complex acts to chaperone the proteins from the ribosome to the ER membrane insertion machinery (42, 43). It seems plausible that when IP$_3$R1 is absent, the lack of an appropriate docking site for newly synthesized Bok at the ER membrane means that its insertion into the ER membrane is impaired and that it is diverted to the UPP. Such a mechanism that causes the destruction of free Bok is entirely consistent with the observation that essentially all cellular Bok is bound to IP$_3$Rs. Other Bcl-2 protein family members are also targeted by the UPP (44–47), and

it will be interesting to see if they too are subject to a similar kind of "quality control."

It is intriguing that the 23- and 21-kDa Bok variants appear to originate from alternative translational initiation at Met^1 and Met^{15}. It remains possible that proteolysis could account for the 21-kDa variant, but that seems unlikely because mutation of Met^{15} to Ala completely blocks formation of the 21-kDa band and highly Met-specific endoproteases are not known. Alternative translational initiation could result from "leaky scanning" (33, 34), although why this should occur for Bok mRNA is unclear, since the Kozak consensus sequence around Met^1 (GCCAUGG) is ideal (33, 34). It is equally puzzling that exogenous 3F-Bok generates the 21- and 23-kDa variants, as well as the full-length construct at 27 kDa, since this indicates that "leaky scanning" also occurs at the initiation codon at the start of the 3× FLAG region, again despite an ideal Kozak sequence (ACCAUGG). Perhaps secondary structure of Bok mRNA disrupts the scanning process (33, 34). Whatever their origin, both forms of Bok bind to IP_3R1 (*e.g.* Fig. 1), which is to be expected given that the binding is mediated by the BH4 domain (residues 34–39). However, it is likely that the two forms will have different properties, since full-length (23 kDa) Bok can be phosphorylated at Ser^8 (37), which is absent from the 21-kDa form.

The region to which Bok binds appears to be a flexible, unstructured, surface-exposed loop within the ARM3 domain of IP_3Rs (14, 16). The ARM3 domain is composed of an ensemble of 6 armadillo repeats, and together with the ARM 1 and 2 domains, is thought to form a flexible, solenoid-like structure that facilitates propagation of ligand-evoked signals to the channel pore (16). The ARM3 domain is also a regulatory hotspot, containing sites for phosphorylation, ATP binding, Ca^{2+} binding, caspase-3 cleavage, and ubiquitination (15, 16, 48). Proteolysis within the ARM3 domain has recently been suggested to provide a novel mode of IP_3R regulation (49) and it is intriguing that such proteolysis is inhibited by Bok, most likely because of steric hindrance (14). In view of the ability of Bcl-2 to regulate IP_3R channel activity (17–20), and the recently described findings that Bcl-x_L activates channel gating by interacting with BH3 domain-like helices in the IP_3R C-terminal tail (50), it is somewhat surprising that initial experiments with control and $Bok^{-/-}$ mouse embryonic fibroblasts did not reveal a major effect of Bok on the Ca^{2+}-mobilizing function of IP_3Rs (14). However, a caveat with this study is that the $Bok^{-/-}$ cells have adapted in terms of IP_3R1–3 expression (14) and thus, whether Bok binding to the ARM3 domain directly regulates the Ca^{2+} mobilizing function of IP_3Rs remains to be determined. Another possibility, given the strength of the Bok-IP_3R interaction and that Bok has a TM domain, is that Bok contributes to the structural integrity or stability of IP_3R tetramers. Interestingly, Bok is well expressed in the brain (4, 7, 12) and is enriched in the CA3 region of the hippocampus (51, 52). Our data indicate that in cerebral cortex and hippocampus, Bok is bound to IP_3R1, and in this context, Bok binding should, at minimum, serve to protect IP_3R1 from caspase 3-mediated proteolysis (14).

Bok is widely and highly expressed in mammalian tissues and is well conserved across mammalian species, yet attempts to define its biological role, and in particular the role it is suspected to play in apoptosis, have not led to a clear consensus view (4, 7, 11, 12, 53, 54). This may, in part, be because of the tight binding between Bok and IP_3Rs and the degradation of free Bok by the UPP; in experiments in which exogenous Bok is introduced into cells, the amount of Bok expressed will be limited by the UPP and will vary between cell types because of differences in IP_3R expression (14). Further, it is tempting to speculate that the existence of a cellular mechanism that efficiently destroys free Bok indicates that free Bok is harmful to the cell, and that in experiments in which Bok is overexpressed, apoptosis occurs because UPP-mediated Bok degradation is overwhelmed and free Bok is formed (7–10). This view is supported by our finding that Bok^{L34G} is more pro-apoptotic than Bok^{WT}. Certainly, if the apoptosis seen in Bok overexpression experiments (7–10) is considered to be "non-physiological," it would help to rationalize data showing that there are no major apoptotic deficiencies attributable to Bok in $Bok^{-/-}$ mice (4, 11, 12), or in mice in which Bok is deleted in combination with Bak and Bax (11, 55).

Author Contributions—R. J. H. W. conceived and coordinated the study and wrote the paper with substantial editorial input from J. J. S. J. J. S. performed and analyzed all of the experiments shown, with input from E. J. Z. (Fig. 1) and L. M. S. (Fig. 6). X. H. performed the molecular modeling and MD simulations. F. A. W. created the cell lines used in Fig. 6. J. J. S. and F. A. W. both helped guide the study. All authors reviewed the results and approved the final version of the manuscript.

Acknowledgments—We thank Drs. Richard Kopp and Michael Roe, SUNY Upstate Medical University, for help with the mRNA measurements, Dr Thomas Kaufmann, University of Bern, Switzerland, for providing anti-Bok and the cDNAs for mouse Bok^{WT} and human Bak, Dr. Jan Parys, KU Leuven, Belgium, for providing anti-IP_3R1–3, Dr. Danielle Sliter and Elizabeth Snyder for helpful suggestions.

References

1. Youle, R. J., and Strasser, A. (2008) The BCL-2 protein family: opposing activities that mediate cell death. *Nat. Rev. Mol. Cell Biol.* **9,** 47–59
2. Kelly, P. N., and Strasser, A. (2011) The role of Bcl-2 and its pro-survival relatives in tumourigenesis and cancer therapy. *Cell Death Differ.* **18,** 1414–1424
3. Moldoveanu, T., Follis, A. V., Kriwacki, R. W., and Green, D. R. (2014) Many players in BCL-2 family affairs. *Trends Biochem. Sci.* **39,** 101–111
4. Ke, F., Voss, A., Kerr, J. B., O'Reilly, L. A., Tai, L., Echeverry, N., Bouillet, P., Strasser, A., and Kaufmann, T. (2012) BCL-2 family member BOK is widely expressed but its loss has only minimal impact in mice. *Cell Death Differ.* **19,** 915–925
5. Chi, X., Kale, J., Leber, B., and Andrews, D. W. (2014) Regulating cell death at, on and in membranes. *Biochim. Biophys. Acta* **1843,** 2100–2113
6. Chen, H-C., Kanai, M., Inoue-Yamauchi, A., Tu, H-C., Huang, Y., Ren, D., Kim, H., Takeda, S., Reyna, D. E., Chan, P. M., Ganesan, Y. T., Liao, C-P., Gavathiotis, E., Hsieh, J. J., and Cheng, E. H. (2015) An interconnected hierarchical model of cell death regulation by the BCL-2 family. *Nature Cell Biol.* **17,** 1270–1281
7. Echeverry, N., Bachmann, D., Ke, F., Strasser, A., Simon, H-U., and Kaufmann, T. (2013) Intracellular localization of the BCL-2 family member BOK and functional implications. *Cell Death Differ.* **20,** 785–799
8. Hsu, S. Y., Kaipia, A., McGee, E., Lomeli, M., and Hsueh, A. J. W. (1997) Bok is a pro-apoptotic Bcl-2 protein with restricted expression in reproductive tissues and heterodimerizes with selective anti-apoptotic Bcl-2 family members. *Proc. Natl. Acad. Sci. U.S.A.* **94,** 12401–12406

9. Hsu, S. Y., and Hsueh, A. J. W. (1998) A splicing variant of the Bcl-2 member Bok with a truncated BH3 domain induces apoptosis but does not dimerize with antiapoptotic Bcl-2 proteins *in vitro*. *J. Biol. Chem.* **273,** 30139–30146
10. Inohara, N., Ekhterae, D., Garcia, I., Carrio, R., Merino, J., Merry, A., Chen, S., and Núñez, G. (1998) Mtd, a novel Bcl-2 family member activates apoptosis in the absence of heterodimerization with Bcl-2 and Bcl-xL. *J. Biol. Chem.* **273,** 8705–8710
11. Ke, F., Bouillet, P., Kaufmann, T., Strasser, A., Kerr, J., and Voss, A. K. (2013) Consequences of the combined loss of BOK and BAK or BOK and BAX. *Cell Death Dis.* **4,** e650
12. Carpio, M. A., Michaud, M., Zhou, W., Fisher, J. K., Walensky, L. D., and Katz, S. G. (2015) BCL-2 family member BOK promotes apoptosis in response to endoplasmic reticulum stress. *Proc. Natl. Acad. Sci. U.S.A.* **112,** 7201–7206
13. Zhao, L., and Ackerman, S. L. (2006) Endoplasmic reticulum stress in health and disease. *Curr. Opin. Cell Biol.* **18,** 444–452
14. Schulman, J. J., Wright, F. A., Kaufmann, T., and Wojcikiewicz, R. J. H. (2013) The Bcl-2 protein family member Bok binds to the coupling domain of inositol 1,4,5-trisphosphate receptors and protects them from proteolytic cleavage. *J. Biol. Chem.* **288,** 25340–25349
15. Foskett, J. K., White, C., Cheung, K. H., and Mak, D. O. (2007) Inositol trisphosphate receptor Ca^{2+} release channels. *Physiol. Rev.* **87,** 593–658
16. Fan, G., Baker, M. L., Wang, Z., Baker, M. R., Sinyagovskiy, P. A., Chiu, W., Ludtke, S. J., and Serysheva, I. I. (2015) Gating machinery of $InsP_3R$ channels revealed by electron microscopy. *Nature* **527,** 336–341
17. Rong, Y-P., Aromolaran, A. S., Bultynck, G., Zhong, F., Li, X., McColl, K. S., Matsuyama, S., Herlitze, S., Roderick, H. L., Bootman, M. D., Mignery, G. A., Parys, J. B., De Smedt, H., and Distelhorst, C. W. (2008) Targeting Bcl-2-IP3 receptor interaction to reverse Bcl-2's inhibition of apoptotic calcium signals. *Mol. Cell* **31,** 255–265
18. Distelhorst, C. W., and Bootman, M. D. (2011) Bcl-2 interaction with the inositol 1,4,5-trisphosphate receptor: Role in Ca^{2+} signaling and disease. *Cell Calcium* **50,** 234–241
19. Monaco, G., Decrock, E., Akl, H., Ponsaerts, R., Vervliet, T., Luyten, T., De Maeyer, M., Missiaen, L., Distelhorst, C. W., De Smedt, H., Parys, J. B., Leybaert, L., and Bultynck, G. (2012) Selective regulation of IP_3-receptor-mediated Ca^{2+} signaling and apoptosis by the BH4 domain of Bcl-2 *versus* Bcl-xL. *Cell Death Differ.* **19,** 295–309
20. Lavik, A. R., Zhong, F., Chang, M. J., Greenberg, E., Choudhary, Y., Smith, M. R., McColl, K. S., Pink, J., Reu, F. J., Matsuyama, S., and Distelhorst, C. W. (2015) A synthetic peptide targeting the BH4 domain of Bcl-2 induces apoptosis in multiple myeloma and follicular lymphoma cells alone or in combination with agents targeting the BH3-binding pocket of Bcl-2. *Oncotarget* **6,** 27388–27402
21. Wojcikiewicz, R. J. H. (1995) Type I, II and III inositol 1,4,5-trisphosphate receptors are unequally susceptible to down-regulation and are expressed in markedly different proportions in different cell types. *J. Biol. Chem.* **270,** 11678–11683
22. Pearce, M. M. P., Wang, Y., Kelley, G. G., and Wojcikiewicz, R. J. H. (2007) SPFH2 mediates the endoplasmic reticulum-associated degradation of inositol 1,4,5-trisphosphate receptors and other substrates in mammalian cells. *J. Biol. Chem.* **282,** 20104–20115
23. Bultynck, G., Szlufcik, K., Kasri, N. N., Assefa, Z., Callewaert, G., Missiaen, L., Parys, J. B., and De Smedt, H. (2004) Thimerosal stimulates Ca^{2+} flux through inositol 1,4,5-trisphosphate receptor type 1, but not type 3, via modulation of an isoform-specific Ca^{2+}-dependent intramolecular interaction. *Biochem. J.* **381,** 87–96
24. Lu, J. P., Wang, Y., Sliter, D. A., Pearce, M. M. P., and Wojcikiewicz, R. J. H. (2011) RNF170, an endoplasmic reticulum membrane ubiquitin ligase, mediates inositol 1,4,5-trisphosphate receptor ubiquitination and degradation. *J. Biol. Chem.* **286,** 24426–24433
25. Wright, F. A., Lu, J. P., Sliter, D. A., Dupré, N., Rouleau, G. A., and Wojcikiewicz, R. J. H. (2015) A point mutation in the ubiquitin ligase RNF170 that causes autosomal dominant sensory Ataxia destabilizes the protein and impairs inositol 1,4,5-trisphosphate receptor-mediated Ca^{2+} signaling. *J. Biol. Chem.* **290,** 13948–13957
26. Matsuda, T., and Cepko, C. L. (2004) Electroporation and RNA interference in the rodent retina *in vivo* and *in vitro*. *Proc. Natl. Acad. Sci. U.S.A.* **101,** 16–22
27. Ran, F. A., Hsu, P. D., Wright, J., Agarwala, V., Scott, D. A., and Zhang, F. (2013) Genome engineering using the CRISPR-Cas9 system. *Nat. Protoc.* **8,** 2281–2308
28. Livak, K. J., and Schmittgen, T. D. (2001) Analysis of relative gene expression data using real-time quantitative PCR and the $2^{-\Delta\Delta CT}$ method. *Methods* **25,** 402–408
29. Sali, A., and Blundell, T. L. (1993) Comparative protein modelling by satisfaction of spatial restraints. *J. Mol. Biol.* **234,** 779–815
30. Smith, C. A., and Kortemme, T. (2008) Backrub-like backbone simulation recapitulates natural protein conformational variability and improves mutant side-chain prediction. *J. Mol. Biol.* **380,** 742–756
31. Hess, B., Kutzner, C., van der Spoel, D., and Lindahl, E. (2008) GRGMACS 4: algorithms for highly efficient, load-balanced, and scalable molecular simulation. *J. Chem. Theory Computat.* **4,** 435–447
32. Hornak, V., Abel, R., Okur, A., Strockbine, B., Roitberg, A., and Simmerling, C. (2006) Comparison of multiple Amber force fields and development of improved protein backbone parameters. *Proteins* **15,** 712–725
33. Kozak, M. (1991) An analysis of vertebrate mRNA sequences: Intimations of translational control. *J. Cell Biol.* **115,** 887–903
34. Kochetov, A. V. (2008) Alternative translation start sites and hidden coding potential of eukaryotic mRNAs. *BioEssays* **30,** 683–691
35. Pace, C. N., and Scholtz, J. M. (1998) A helix propensity scale based on experimental studies of peptides and proteins. *Biophys. J.* **75,** 422–427
36. Monaco, G., Decrock, E., Nuyts, K., Wagner, L. E., II., Luyten, T., Strelkov, S. V., Missiaen, L., De Borggraeve, W. M., Leybaert, L., Yule, D. I., De Smedt, H., Parys, J. B., and Bultynck, G. (2013) α-Helical destabilization of the Bcl-2-BH4-domain peptide abolishes its ability to inhibit the IP_3 receptor. *PLOS One.* **8,** e73386
37. Miller, R. L., Sandoval, P. C., Pisitkun, T., Knepper, M. A., and Hoffert, J. D. (2013) Vasopressin inhibits apoptosis in renal collecting duct cells. *Am. J. Physiol. Renal Physiol.* **304,** F177-F188
38. Kleiger, G., and Mayor, T. (2014) Perilous journey: a tour of the ubiquitin-proteasome system. *Trends Cell Biol.* **24,** 352–359
39. Wang, Q., Liu, Y., Soetandyo, N., Baek, K., Hegde, R., and Ye, Y. (2011) A ubiquitin ligase-associated chaperone holdase maintains polypeptides in soluble states for proteasome degradation. *Mol. Cell* **42,** 758–770
40. Kalbfleisch, T., Cambon, A., and Wattenberg, B. W. (2007) A bioinformatics approach to identifying tail-anchored proteins in the human genome. *Traffic* **8,** 1687–1694
41. Wilfling, F., Weber, A., Potthoff, S., Vögtle, F-N., Meisinger, C., Paschen, S. A., and Häcker, G. (2012) BH3-only proteins are tail-anchored in the outer mitochondrial membrane and can initiate the activation of Bax. *Cell Death Differ.* **19,** 1328–1336
42. Mariappan, M., Li, X., Stefanovic, S., Sharma, A., Mateja, A., Keenan, R. J., and Hegde, R. S. (2010) A ribosome-associating factor chaperones tail-anchored membrane proteins. *Nature* **466,** 1120–1124
43. Kawahara, H., Minami, R., and Yokota, N. (2013) BAG6/BAT3: emerging roles in quality control of nascent polypeptides. *J. Biochem.* **153,** 147–160
44. Breitschopf, K., Haendeler, J., Malchow, P., Zeiher, A. M., and Dimmeler, S. (2000) Post-translational modification of Bcl-2 facilitates its proteasome-dependent degradation: molecular characterization of the involved signaling pathway. *Mol. Cell. Biol.* **20,** 1886–1896
45. Wang. P., Wu, Y., Li, Y., Zheng, J., and Tang, J. (2013) A novel RING finger E3 ligase RNF186 regulate ER stress-mediated apoptosis through interaction with BNip1. *Cell. Signal.* **25,** 2320–2333
46. Rooswinkel, R. W., van de Kooij, B., de Vries, E., Paauwe, M., Braster, R., Verheij, M., and Borst, J. (2014) Antiapoptotic potency of Bcl-2 proteins primarily relies on their stability, not binding selectivity. *Blood* **123,** 2806–2815
47. Carroll, R. G., Hollville, E., and Martin, S. J. (2014) Parkin sensitizes towards apoptosis induced by mitochondrial depolarization through promoting degradation of Mcl-1. *Cell Reports* **9,** 1538–1553
48. Wojcikiewicz, R. J. H., Pearce, M. M. P., Sliter, D. A., and Wang, Y. (2009) When worlds collide: IP_3 receptors and the ERAD pathway. *Cell Calcium* **46,** 147–153
49. Wang, L., Alzayady, K. J., and Yule, D. I. (2015) Proteolytic fragmentation

of inositol 1,4,5-trisphosphate receptors: a novel mechanism regulating channel activity? *J. Physiol.* (in press)
50. Yang, J., Vais, H., Gu, W., and Foskett, J. K. (2016) Biphasic regulation of IP_3 receptor gating by dual Ca^{2+} release channel BH3-like domains mediates Bcl-xL control of cell viability. *Proc. Natl. Acad. Sci. U.S.A.* **113,** E1953–E1962
51. Lein, E. S., Zhao, X., and Gage, F. H. (2004) Defining a molecular atlas of the hippocampus using DNA microarrays and high-throughput *in situ* hybridization. *J. Neurosci.* **24,** 3879–3889
52. Lein, E. S., Callaway, E. M., Albright, T. D., and Gage, F. H. (2005) Redefining the boundaries of the hippocampal CA2 subfield in the mouse using gene expression and 3-dimensional reconstruction. *J. Comp. Neurol.* **485,** 1–10
53. Fernandez-Marrero, Y., Ke, F., Echeverry, *N.,* Bouillet, P., Bachmann, D., Strasser, A., and Kaufmann, T. (2016) Is Bok required for apoptosis induced by endoplasmic reticulum stress? *Proc. Natl. Acad. Sci. U.S.A.* **113,** E492–E493
54. Carpio, M. A., Michaud, M., Zhou, W., Fisher, J. K., Walensky, L. D., and Katz, S. G. (2016) Role of Bok at the intersection of endoplasmic reticulum stress and apoptosis regulation. *Proc. Natl. Acad. Sci. U.S.A.* **113,** E494–E495
55. Ke, F., Grabow, S., Kelly, G. L., Lin, A., O'Reilly, L. A., and Strasser, A. (2015) Impact of the combined loss of BOK, BAX and BAK on the hematopoietic system is slightly more severe than compound loss of BAX and BAK. *Cell Death Dis.* **6,** e1938